NIH Public Access
Author Manuscript
Sci Transl Med. Author manuscript; available in PMC 2014 September 19.

Published in final edited form as:
Sci Transl Med. 2013 November 13; 5(211): 211ra156. doi:10.1126/scitranslmed.3006534.

Restoration of the Unfolded Protein Response in Pancreatic β Cells Protects Mice Against Type 1 Diabetes

Feyza Engin[1], **Alena Yermalovich**[1], **True Nguyen**[1], **Sarah Hummasti**[1], **Wenxian Fu**[2], **Decio L. Eizirik**[3], **Diane Mathis**[2,4], and **Gökhan S. Hotamisligil**[1,4,*]

[1]Department of Genetics and Complex Diseases, Harvard School of Public Health, Boston, MA 02115, USA.

[2]Division of Immunology, Department of Microbiology and Immunobiology, Harvard Medical School, 77 Avenue Louis Pasteur, Boston, MA 02115, USA.

[3]Laboratory of Experimental Medicine, Medical Faculty, Université Libre de Bruxelles, Erasmus Hospital, Campus Erasme, 1070 Brussels, Belgium.

[4]The Broad Institute of Harvard and MIT, Cambridge, MA 02142, USA.

Abstract

Perturbations in endoplasmic reticulum (ER) homeostasis can evoke stress responses leading to aberrant glucose and lipid metabolism. ER dysfunction is linked to inflammatory disorders, but its role in the pathogenesis of autoimmune type 1 diabetes (T1D) remains unknown. We identified defects in the expression of unfolded protein response (UPR) mediators ATF6 (activating transcription factor 6) and XBP1 (X-box binding protein 1) in β cells from two different T1D mouse models and then demonstrated similar defects in pancreatic β cells from T1D patients. Administration of a chemical ER stress mitigator, tauroursodeoxycholic acid (TUDCA), at the prediabetic stage resulted in a marked reduction of diabetes incidence in the T1D mouse models. This reduction was accompanied by (i) a significant decrease in aggressive lymphocytic infiltration in the pancreas, (ii) improved survival and morphology of β cells, (iii) reduced β cell apoptosis, (iv) preserved insulin secretion, and (v) restored expression of UPR mediators. TUDCA ′s actions were dependent on ATF6 and were lost in mice with β cell-specific deletion of *ATF6*.

*Corresponding author. ghotamis@hsph.harvard.edu.

SUPPLEMENTARY MATERIALS

www.sciencetranslationalmedicine.org/cgi/content/full/5/211/211ra156/DC1

Materials and Methods

Fig. S1. Specific alterations of the UPR mediators in the islets of NOD mice.

Fig. S2. Specific alterations of Glut2 and Keapl expression in the islets of NOD mice.

Fig. S3. Dysregulation of the molecules critical in the UPR in the islets of male T1D patients.

Fig. S4. Immunophenotyping of splenocytes of NOD mice after TUDCA treatment.

Fig. S5. Immunophenotyping of pancreatic lymph nodes of NOD mice after TUDCA treatment.

Fig. S6. Deletion of ATF6 branch of the UPR in β cells in vivo.

Author contributions: F.E. designed and performed all in vitro and in vivo experiments, established staining protocols for both human and mouse samples, analyzed the data, and helped write the manuscript. A.Y. and T.N. contributed to in vivo experiments and immunostainings. S.H. generated ATF6-targeting vector. W.F. helped with immunophenotyping of the mice. D.L.E. supervised the in vitro studies and edited the manuscript. D.M. supervised the immunological analyses and edited the manuscript. G.S.H. supervised the in vitro and in vivo studies and statistical analyses, analyzed the data, and wrote the manuscript.

Competing interests: The authors declare that they have no competing interests.

NIH-PA Author Manuscript
NIH-PA Author Manuscript
NIH-PA Author Manuscript

NIH-PA Author Manuscript

NIH-PA Author Manuscript

NIH-PA Author Manuscript

These data indicate that proper maintenance of the UPR is essential for the preservation of β cells and that defects in this process can be chemically restored for preventive or therapeutic interventions in T1D.

INTRODUCTION

Type 1 diabetes (T1D) results from the immune-mediated destruction of insulin-producing β cells in the hormone-generating islets of Langerhans in the pancreas. Loss of pancreatic β cells leads to a decrease in insulin production, unsuppressed glucose production, and hyperglycemia (1,2). The prevalence of T1D in humans between the ages of 0 and 19 years was reported to be 1.7 per 1000 and has been rising globally and by as much as 5.3% annually in the United States (3). The initial signals that trigger autoimmunity and the intracellular mediators that lead to destruction of β cells in T1D remain poorly understood, a situation that hampers the development of targeted therapies for the disease. Growing experimental evidence suggests that dysregulation of the endoplasmic reticulum (ER) responses contributes to T1D pathogenesis through multiple potential mechanisms that eventually lead to β cell demise (2, 4–6). For example, acute and chronic stimulation of β cells by nutrients such as glucose, arginine, or lipids induces the production of large amounts of insulin, which places a continuous demand on the ER for proper protein synthesis, folding, trafficking, and secretion. When the folding capacity of the ER is exceeded, misfolded or unfolded proteins accumulate in the ER lumen, triggering the unfolded protein response (UPR). The UPR is an integrated response program that reduces translation, increases chaperone availability, and enhances the degradation of misfolded proteins in an attempt to restore ER homeostasis.

Although physiological stimulation of the UPR may be beneficial for β cell function and acute adaptation to stress, under pathological conditions severe or prolonged ER stress hinders β cell function and survival (7, 8). In experimental animal models and in humans, mutations in genes critical for ER function result in β cell failure and severe early-onset diabetes (9–17). In fact, misfolded insulin alone can cause diabetes in both mice and humans (18–23).

Proinflammatory cytokines produced by islet-infiltrating immune cells also lead to β cell destruction by direct cytotoxicity, inducing expression of FAS [tumor necrosis factor (TNF) receptor superfamily, member 6], and enhancement of immune recognition (4). Putative inflammatory mediators of β cell loss in T1D, such as interleukin-1β (IL-1β), TNF-α, and interferon-γ (IFN-γ), were all shown to induce ER stress through multiple mechanisms (24, 25), leading to the depletion of ER calcium, dysfunction of ER chaperones, and a severe disruption in ER homeostasis (26, 27). Hence, cytokine-induced alterations in ER function can affect cell adaptation and amplify proapoptotic pathways. Reciprocally, chronic ER stress can engage stress and inflammatory pathways through activation of c-Jun N-terminal kinase (JNK), inhibitor of nuclear factor κB kinase (IKK), and protein kinase R (PKR), and this low-grade chronic inflammation may also contribute to eventual islet destruction (6,28,29). Indicators of ER stress are present in inflamed islets of both diabetes-prone non-obese diabetic (NOD) mice (30) and patients with T1D (31).

NIH-PA Author Manuscript

NIH-PA Author Manuscript

NIH-PA Author Manuscript

Viral infection, environmental toxins, chronic inflammation, abnormal protein folding, and a surplus of nutrients all can cause ER stress and trigger the UPR (32). In addition to the prosurvival aspects of the UPR described above, when stress is prolonged and unresolved, the UPR can engage apoptotic pathways. The canonical UPR operates through inositol-requiring protein 1 (IRE1), protein kinase RNA-like ER kinase (PERK), and activating transcription factor 6 (ATF6), all of which are localized in the ER membrane and respond to stress by relaying signals from the ER to the cytoplasm and nucleus. Recent studies elucidated the importance of ER stress and the beneficial effects of restoring organelle function through chemical and lipid chaperones in the context of obesity, insulin resistance, type 2 diabetes (T2D), and atherosclerosis (33, 34).

Unlike T2D, however, it remains unclear whether ER stress and components of the UPR play a mechanistic role in the steps leading to pancreatic β cell dysfunction and death in T1D. Here, we investigated the role of the UPR and its components during the pathogenesis of T1D in mouse models and in human subjects. Furthermore, we explored the prospect of UPR-modulating chemical chaperones as potential therapeutic agents in the preservation of β cell function and survival in T1D.

RESULTS

To investigate whether an aberrant UPR plays a role during the natural course of T1D, we first examined the expression patterns of key UPR mediators, sXBP1 (spliced X-box binding protein 1) and ATF6, in pancreata of NOD mice at 3, 5, 7, 9, and 13 weeks of age ($n = 14$ for each group). For immunohistochemical analysis of the pancreatic islets, we used both commercially available and in-house antibodies against ATF6 and sXBP1, after validating their specificities by lack of staining in the pancreatic sections of mice with targeted null mutations in these genes (fig. S1, A and B). Expression of ATF6 in the β cells of the pancreatic islets of NOD mice showed a slight increase from 3 to 5 weeks of age; however, there was a sharp decline in ATF6 immunostaining of the islets starting at week 7, which became more pronounced at 13 weeks of age (Fig. 1, A and C). sXBP1 expression exhibited a somewhat different expression pattern compared with that of ATF6: It was detected at low levels at 3 weeks of age but showed a significant increase at 5 weeks of age (Fig. 1, B and D). sXBP1 expression started to decline during weeks 7 and 9, with the greatest decline observed at 13 weeks of age (Fig. 1B). Insulin staining intensity in these islets remained the same until 7 weeks, but showed a mild decrease at 9 and 13 weeks of age (Fig. 1E). Plasma insulin levels were also maintained through 7 weeks of age (Fig. 1F).

To examine alterations in the third branch of the UPR, we stained the same pancreatic sections with an antibody to phosphorylated eukaryotic translation initiation factor 2A (phospho-eIF2α), which indicates activation of PERK and subsequent attenuation of translational initiation. Although phospho-eIF2α staining was below detection in most β cells, islet non-β cells exhibited detectable signals (fig. S1C). Phospho-eIF2α staining markedly decreased at 5 weeks of age and then significantly increased at 7 weeks. Phospho-eIF2α staining through 9 and 13 weeks of age remained similar in β cells to the initial levels observed at 3 weeks of age (fig. S1, C and D). We also examined Glut2, the major glucose transport protein in murine β cells, and Keap1, a transcription factor that regulates

NIH-PA Author Manuscript

NIH-PA Author Manuscript

NIH-PA Author Manuscript

antioxidant genes (35), as additional controls. Although Glut2 staining showed a clear increase in β cells already at 5 weeks of age, Keap1 immunostaining remained the same throughout the time course studied in NOD islets (fig. S2, A to D). These results indicate that the UPR is modulated during diabetes progression in the β cells of NOD mice and precedes the decline in β cell number and function and the emergence of frank diabetes, which is usually observed after 12 weeks of age.

To explore whether a defective UPR is a common phenomenon of T1D, we also examined the expression of UPR markers in the islets of an independent diabetic mouse model induced by viral infection (36). Similar to the observations in NOD mice, the expression of both ATF6 and sXBP1 was severely defective in the RIP-LCMV-GP (rat insulin promoter-lymphocytic choriomeningitis virus-glycoprotein) model preceding the onset of hyperglycemia (fig. S2, E and F). These data indicate that failure of the proresolution functions of the UPR in T1D models is related to impaired functions of ATF6 and XBP1. Furthermore, these observations suggest that a dysregulated UPR may contribute to the pathogenesis of immune-mediated diabetes in mouse models.

To evaluate the expression of UPR markers in human T1D patients, we obtained pancreatic sections from control ($n = 6$) and diabetic ($n = 10$) individuals [from the Network for Pancreatic Organ Donors with Diabetes (nPOD)] (Table 1) and performed immunofluorescence analysis of ER stress markers in these samples. These data also supported the presence of ER stress indicators in the initial stages of disease, which markedly declined later on (Fig. 2). When the data from all subjects were combined and quantitated, we observed significantly reduced ATF6 (Fig. 2, A and D) and sXBP1 (Fig. 2, B and E) staining intensity in insulin-positive β cells (Fig. 2C) of subjects with diabetes compared with healthy controls. The expression of insulin, ATF6, and sXBP1 was also quantified in controls and in patients individually grouped according to time of diagnosis (indicated by years) (fig. S3, A to C). Representative stainings are shown in female (Fig. 2, A and B) and male (fig. S3, D and E) control and diabetic subjects. This pattern of defective ATF6 and sXBP1 expression was more striking in female patients who had diabetes for 8 to 20 years than in male patients, whose staining pattern was milder but still present. Similar to what we have observed in animal models, these results demonstrate that the ATF6 and XBP1 branches of the UPR are down-regulated in β cells from subjects with diabetes, and thus that these pathways may be important for disease pathogenesis.

In experimental models of both T2D and atherosclerosis, chemical chaperones such as taurine-conjugated ursodeoxycholic acid (TUDCA) and phenyl butyric acid reduce ER stress and alleviate disease symptoms (34, 37, 38). These chemical chaperones also increase insulin sensitivity in obese and insulin-resistant subjects and provide protection against lipid-induced β cell dysfunction in humans (39, 40). We hypothesized that by increasing ER capacity, improving folding defects, or promoting the prosurvival or adaptive effects of the UPR, chemical chaperones might also protect pancreatic β cells in T1D. To test this hypothesis, we administered TUDCA to both NOD and RIP-LCMV-GP mice at 250 mg/kg twice daily via intraperitoneal injections for 20 and 2 weeks, respectively, and monitored body weight and blood glucose levels weekly. TUDCA treatment resulted in a striking reduction in diabetes incidence in both the NOD (44 versus 11%) ($P < 0.05$, Kaplan-Meier

NIH-PA Author Manuscript

NIH-PA Author Manuscript

NIH-PA Author Manuscript

estimate) and RIP-LCMV-GP (100 versus 40%) ($P < 0.05$, χ^2 test) models (Fig. 3, A and B). To investigate the dose responsiveness of the TUDCA effect, we administered TUDCA (100, 50, and 25 mg/kg per day) to the RIP-LCMV-GP model and followed the diabetes incidence in these animals by measuring blood glucose levels twice a week for 2 weeks. There was a clear dose-dependent beneficial effect of this chaperone (Fig. 3C).

TUDCA-treated NOD mice preserved serum insulin at the level observed in vehicle-treated animals, which did not progress to diabetes (Fig. 3D) (Veh-D versus TUDCA, $P < 0.0001$ by Student's *t* test). Histological analysis of pancreatic sections demonstrated noticeably reduced aggressive insulitis in TUDCA-treated mice compared with vehicle-treated diabetic (Veh-D) NOD mice (Fig. 3E). Furthermore, islets from mice receiving TUDCA remained largely intact despite the presence of inflammatory cells in both the NOD and RIP-LCMV-GP models (Fig. 3, E and F). These results indicate that treatment with TUDCA renders the β cells of diabetes-prone mice significantly more resistant to aggressive immune cell infiltration than those of untreated animals. This is reflected in increased serum insulin, markedly preserved islet architecture, and reduced diabetes incidence.

It is possible that systemic administration of TUDCA could lead to alterations in immune phenotype through its antiapoptotic effects or other unknown mechanisms. To address this issue, we treated 10-week-old, normoglycemic female NOD mice with either phosphate-buffered saline (PBS) (vehicle) or TUDCA (500 mg/kg per day) for 4 weeks and collected the spleen, pancreas, and pancreatic lymph nodes for immunophenotyping via flow cytometry. T1D is a T cell-dominated autoimmune disease, although various types of other immune cells, including B and myeloid cells, are also involved (41). $CD4^+CD25^+Foxp3^+$ T regulatory cells (T_{regs}) play an important role in controlling diabetes progression both in mouse models and in human T1D patients (42–44). TUDCA treatment did not cause alterations in the percentages of $CD4^+$ or $CD8^+$ T cells (Fig. 4, A to C), T_{regs} (Fig. 4, D and E), or B cells (Fig. 4, F and G) locally in the pancreas. There were also no differences in the corresponding cell populations in lymph nodes or spleens from TUDCA- versus vehicle-treated mice (figs. S4 and S5). Hence, systemic administration of TUDCA treatment did not affect the relative representation of immune cell populations critically implicated in T1D. On the other hand, TUDCA-treated NOD mice showed less severe islet infiltration by immune cells, suggesting that better islet function and survival led to less recruitment of immune cells to the islets, perhaps reflecting less antigen presentation.

In light of these data, we next focused on exploring the mechanisms underlying the beneficial effects of TUDCA. We first examined UPR markers in β cells for their potential alterations in 30-week-old vehicle- or TUDCA-treated animals. In both the RIP-LCMV-GP and NOD models, there was a striking loss of ATF6 expression in β cells upon emergence of diabetes compared with controls; this decrease in ATF6 expression was, to a great extent, maintained in TUDCA-treated animals in both models of disease (Fig. 5, A to D). This prompted us to investigate whether TUDCA could cause relevant molecular changes in normoglycemic mice before the onset of diabetes. For this purpose, we administered TUDCA for 4 weeks to 10-week-old NOD mice. Insulitis scoring was performed on hematoxylin and eosin (H&E)-stained pancreatic step sections ($n = 8$ each group) to explore the extent of inflammation in the islets (Fig. 5E). Quantification revealed an increase in the

NIH-PA Author Manuscript

NIH-PA Author Manuscript

NIH-PA Author Manuscript

percentage of islets without any insulitis in TUDCA-treated mice in comparison with pancreatic sections of vehicle (PBS)-treated animals (Fig. 5F). Furthermore, the number of islets with severe insulitis was significantly decreased in the TUDCA-treated group compared with controls (Fig. 5G). In addition to reducing ER stress in β cells, the decreased islet inflammatory cell infiltration mediated by TUDCA treatment diminished cell death, which resulted from decreased inflammatory insult; consistent with this notion, we detected a fivefold reduction in TUNEL (terminal deoxynucleotidyl transferase-mediated deoxyuridine triphosphate nick-end labeling)–positive cells in the islets of the TUDCA-treated animals (n = 8, $P < 0.001$ by Student's *t* test) (Fig. 5H). To investigate whether 4 weeks of TUDCA treatment altered the expression of UPR markers in prediabetic NOD mice, we grouped the pancreata from vehicle- and TUDCA-treated animals according to their insulitis scoring and stained the pancreatic sections with sXBPI and ATF6 antibodies. Although the expression of these UPR mediators was substantially down-regulated in β cells of the vehicle-treated mice that exhibited a more aggressive inflammatory phenotype (Veh*), the expression of these markers in TUDCA-treated islets was indistinguishable from that in the vehicle-treated animals with a low degree of inflammation (Fig. 5,I to L). These data indicate that TUDCA preserves the expression of key UPR components in β cells, likely by increasing ER capacity and leading cells toward a prosurvival fate rather than a proapoptotic one.

We also examined whether TUDCA could affect β cell survival in vivo in the RIP-LCMV-GP model of T1D. TUNEL staining of pancreatic sections indicated a nearly fivefold decrease in islet cell death in TUDCA-treated RIP-LCMV-GP mice, compared with vehicle-treated animals, indicating that TUDCA treatment reduces apoptosis in β cells (Fig. 6A). We directly tested this possibility in a mouse insulin-producing cell line (Min6) to study the impact of TUDCA on prolonged ER stress– induced β cell death in vitro. Tunicamycin treatment of these cells induced death, as evidenced by significantly increased TUNEL positivity (Fig. 6B). This ER stress–induced increase in cell death was markedly reversed by TUDCA exposure (Fig. 6B). At the molecular level, the expression levels of p-JNK, CCAAT/enhancer-binding protein homologous protein (CHOP), cleaved poly(adenosine diphosphate–ribose) polymerase (PARP), and caspase-3 proteins were significantly increased upon tunicamycin treatment of Min6 cells, but these effects were reversed by TUDCA treatment (Fig. 6C). Local inflammatory cytokines produced by infiltrating lymphocytes may also contribute to ER stress or aggravate β cell apoptotic outcomes. To test this possibility, we treated Min6 cells with a cytokine cocktail (TNF-α + IFN-γ + IL-1β) alone or together with a chemical ER stress inducer, thapsigargin, and examined cell viability. Treatment of the cells with thapsigargin or the cytokine mixture caused a decrease in cell viability (Fig. 6, D and E). Further treatment of the thapsigargin-treated cells with TUDCA resulted in a small but significant protection against cell death (Fig. 6, D and E). These data support the hypothesis that TUDCA's impact on T1D may be related to its ability to increase β cells' endurance for immune-mediated dysregulation of the UPR

We next used a molecular approach to modulate adaptive ER responses and study the impact on β cell survival and function. We focused on ATF6 manipulation because this branch of the UPR is markedly suppressed in β cells in disease models (as shown in Figs. 1A and 5C).

NIH-PA Author Manuscript

NIH-PA Author Manuscript

NIH-PA Author Manuscript

For this purpose, Min6 cells were stably transduced with a lentiviral construct in which the expression of the *ATF6* was under the control of doxycycline. In this system, thapsigargin or cytokine treatment resulted in a significant decrease in cell viability and an increase in the expression of the proapoptotic transcription factors CHOP and caspase-3. This increase was partially reversed upon doxycycline-induced ATF6 expression (Fig. 6, F to H). We also tested whether higher levels of ATF6 potentiated TUDCA's ability to protect Min6 cells against death. There was a statistically significant increase in cell viability in ATF6-expressing cells (Fig. 6I), although this was of small magnitude (15 versus 23%) at the dose of TUDCA tested (30 μM). TUDCA treatment restored insulin secretion to a significantly greater extent in ATF6-overexpressing Min6 cells exposed to thapsigargin (Fig. 6J). At this low dose, however, TUDCA failed to protect wild-type Min6 cells against thapsigargin-induced decrease in insulin secretion under low- and high-glucose conditions (Fig. 6J). On the other hand, TUDCA significantly restored glucose-induced insulin secretion (GSIS) in cells expressing exogenous ATF6 (Fig. 6J). These results suggest that ATF6 expression is critical for the beneficial effects of TUDCA on cell viability and insulin secretion in β cells.

We reasoned that if TUDCA is acting through ATF6 to generate its protective effects against T1D, it should fail to exhibit these activities in the absence of ATF6 in vivo. To test this hypothesis, we produced a mouse model of ATF6 deficiency in β cells (Fig. 7A) using a tamoxifen-inducible, Cre-mediated recombination system driven by the rat insulin 2 promoter, and demonstrated specific loss of ATF6 in β cells using immunofluorescence (Fig. 7, B and C). We crossed these animals into the C57BL/6J genetic background and with the RIP-LCMV-GP mice (ATF6-β-deficient mice). Mice with heterozygous or homozygous ATF6 deletions in β cells developed normally and showed body weights similar to those of their respective controls (fig. S6A). These mice were slightly more insulin-sensitive and exhibited a lower insulin secretion curve in the GSIS assay (fig. S6, B to D). To determine whether TUDCA's antiapoptotic effects on β cells were altered in the absence of ATF6, we isolated pancreatic islets from wild-type and ATF6-β-deficient mice and treated the islets in culture with thapsigargin in the presence or absence of TUDCA (fig. S6E). Al-though TUDCA significantly protected wild-type islets from apoptosis, it failed to show any preventive activity against the already increased death in ATF6-deficient primary islets (fig. S6E). These data suggest that the antiapoptotic effects of TUDCA in β cells require ATF6.

Finally, we asked whether this mechanism is also in place in the context of an in vivo model of T1D. For this, we induced diabetes in β cell-specific ATF6α-deficient mice and ATF6 wild-type controls that had been crossed with the RIP-LCMV-GP transgenic model by LCMV administration in the presence or absence of TUDCA treatment (Fig. 7D). In the vehicle-treated controls, there was no difference in the incidence of LCMV-induced diabetes between the ATF6α-deficient and ATF6 wild-type control mice (Fig. 7D). However, although TUDCA treatment significantly reduced diabetes incidence in mice with intact ATF6 (66 versus 100%), its protective effects were completely lost in mice with β cell-specific ATF6α deficiency (Fig. 7D). In wild-type mice, TUDCA treatment resulted in significantly increased β cell insulin staining intensity (Fig. 7E), higher sXBP1 protein levels (Fig. 7F), and a lower number of apoptotic cells (Fig. 7G). All of these restorative TUDCA activities were absent from the islets of β cell-specific ATF6-deficient mice (Fig. 7, E to G).

NIH-PA Author Manuscript

NIH-PA Author Manuscript

NIH-PA Author Manuscript

Together, these data demonstrate that TUDCA protects β cells against ER stress-induced death as well as against in vivo development of immune-mediated diabetes in an ATF6-dependent manner.

DISCUSSION

There is increasing evidence in T1D that stress mechanisms intrinsic to β cells are critical for the demise of these cells in the presence of autoimmunity (4). This property is also evidenced by the limited long-term utility of immunosuppressive therapeutic strategies in T1D (45). Therefore, a mechanistic understanding of β cell-specific stress mechanisms and the development of therapeutic tools to target these pathways carry important translational implications.

In recent years, ER stress and related signaling networks have been implicated in the survival of β cells. For example, recent findings indicate that markers of the UPR are expressed in inflamed islets of both diabetes-prone NOD mice (30) and patients with T1D (31). However, it remains to be determined whether ER stress contributes to the pathogenesis of T1D or is an epiphenomenon of the local inflammation and mechanisms that determine the outcome of the UPR during insulitis. It is also unclear whether the ER can be targeted for the prevention and treatment of T1D in experimental models and in humans.

Here, we demonstrate a progressive loss of UPR mediator expression before the onset of diabetes in NOD mice. Two key transcriptional regulators of adaptive UPR, sXBP1 and ATF6, were severely diminished in β cells at the onset of diabetes in NOD and RIP-LCMV transgenic mice. The third canonical branch of the UPR regulated by PERK showed an initial up-regulation (as assessed by the expression of phopspho-eIF2α) followed by stability in non-β cells of the islets of both mouse models of T1D. UPR indicators ATF6 and sXBP1 were similarly down-regulated in pancreatic sections of T1D humans. Hence, deficiency of these UPR branches involved in relevant cell-adaptive mechanisms correlates with β cell death and insulin deficiency in both experimental models and human T1D. These findings suggest that mitigation of ER stress, increase in ER capacity, and promotion of prosurvival outcomes of the UPR might be important for maintaining β cell homeostasis and survival when under an autoimmune attack Consistent with this hypothesis, our results indicate that TUDCA, a molecule that modulates the UPR, significantly reduced the incidence of diabetes, improved insulin secretion and β cell morphology, and hindered the autoimmune attack of pancreatic islets in mouse models of T1D when applied at the prediabetic stage. In addition, administration of TUDCA prevented the loss of expression of the critical UPR regulators ATF6 and XBP1.

Our histological studies indicate that highly secretory β cells need an active and well-balanced UPR to function properly, especially when faced with proinflammatory signals that may lead to ER stress. The UPR is a dynamic cellular response integrated to inflammatory cues, and when key adaptive mechanisms fail, the UPR provides signals that may cause a shift from a compensatory to an apoptotic outcome (32). Consistent with this notion, islets from alloxan-induced diabetes-resistant (ALR/LT) mice, whose genomes show 70% homology to the NOD genome but are resistant to autoimmune destruction (46, 47), have

NIH-PA Author Manuscript

NIH-PA Author Manuscript

NIH-PA Author Manuscript

increased expression of molecules critical for adapting to ER stress, including heat shock proteins, glucose-regulated protein 94 (GRP94), GRP78, protein disulfide isomerase, and calreticulin (47). To date, various branches of the UPR have been implicated in β cell biology and pathology. For example, a loss-of-function mutation in *Perk* causes permanent neonatal diabetes (Wolcott-Rallison syndrome) in humans and mice (9, 11). Another mediator of the UPR, IRE1, is required for insulin biosynthesis in vitro and in vivo (15). However, the function and significance of the third branch of the UPR, namely, the ATF6 axis, in diabetes remains largely unknown. As discussed above, prolonged ER stress can cause a switch from adaptive to proapoptotic UPR, and defective UPR activity during chronic stress may serve as a critical point for cells to switch from homeostasis to malfunction and apoptosis (48, 49). During prolonged ER stress, ATF6 expression decreases in some human cells, suggesting that attenuated ATF6 signaling creates an imbalance between proapoptotic and adaptive outcomes (49). In line with this interpretation, inhibition of ATF6 through a proteinase inhibitor or via a dominant-negative mutant of ATF6 impairs cardiac function in mice (50), whereas mice that express a constitutively active version of ATF6 have improved cardiac function after myocardial infarction compared with wild-type litter-mates (50). This beneficial effect of ATF6 was confirmed in ischemia and reperfusion animal models (51). A similar loss of ATF6 activity has been observed in the liver of obese and T2D animal models, leading to dysregulated hepatic glucose production (52).

In β cells, suppression of ATF6 expression decreases viability even in the absence of ER stress (53). Our findings suggest that in pathological conditions characterized by chronic ER stress, diminished ATF6 or sXBP1 activity inhibits adaptive responses in favor of cell death. If this hypothesis is correct, appropriate complementation of the diminished branches of UPR activity may restore homeostasis, a postulate that has remained untested in β cells in vivo. Our observations demonstrated markedly diminished ATF6 activity in β cells of mice and humans with T1D. However, immunostaining results in human cadaver samples must be viewed with caution because the small sample number presents limitations in making precise comparisons, and samples can exhibit variations as a result of the procurement processes.

To investigate the impact of decreased ATF6 expression and the role of the corresponding UPR branch in mediating chemical chaperone activity, we generated an inducible model of ATF6 deficiency in β cells. Consistent with previous in vitro findings, deletion of the *ATF6* in β cells of RIP-LCMV-GP mice increased the rate of β cell apoptosis as studied in isolated islets (fig. S6E). Although TUDCA was effective in protecting against ER stress-induced death and loss of function in cultured β cell systems, no such protective effect was evident in β cells that lacked ATF6. Heterozygous or homozygous deletion of *ATF6* from β cells did not alter glucose homeostasis or β cell health, whereas β cell–specific deletion of *ATF6* abrogated the protective effects of TUDCA against T1D in the RIP-LCMV model. These in vitro and in vivo observations demonstrate that TUDCA improves β cell survival in the context of an immune attack, at least in part by restoring ATF6. In addition to the important implications for T1D, our findings also provide a molecular mechanism underlying TUDCA action, which is ATF6-dependent in vitro and in vivo.

NIH-PA Author Manuscript

NIH-PA Author Manuscript

NIH-PA Author Manuscript

There are presently no effective regimens for prevention or etiologically oriented treatment of T1D (54, 55). Detection of multiple circulating islet autoantibodies can identify individuals at high risk for development of T1D (56, 57). This capability emphasizes the need for safe and effective approaches to decrease progressive β cell loss and prevent or delay clinical disease. Our data support the possibility that ER-modifying agents such as TUDCA might be used for this purpose in high-risk, autoantibody-positive individuals and perhaps in recently diagnosed T1D patients. TUDCA is an approved drug for human use in some cases of liver disease with no major side effects (58, 59). Administration of TUDCA and other chemical chaperones increases insulin sensitivity in obese humans and in rodent models of T2D (39, 40), suggesting that ER stress can be similarly ameliorated in both species. Finally, most existing therapeutic strategies against T1D involve targeting the immune response (45, 60). Our results support the notion of β cell preservation through the use of TUDCA or potentially other ER-modulating agents as an alternative translational strategy.

MATERIALS AND METHODS

Study design

The overall objective of this project was to study β cell ER stress and the UPR in the context of autoimmune diabetes. To do this, we examined the expression patterns of molecules critical in the UPR in the islets of NOD mice and human patients with T1D. We then treated two different T1D animal models with a chemical chaperone, TUDCA, to alleviate ER stress in these mice. We performed in vitro and in vivo analyses to get insight into the function of TUDCA in β cell survival and function. Insulitis scoring and TUNEL assays were performed in a blinded manner with coded labels. In vitro experiments were repeated at least three times. Except in the study where NOD mice were treated with TUDCA for 20 weeks, in vivo experiments were also repeated at least three times.

Mouse models

The animal care and experimental procedures were performed with approval from the animal care committees of Harvard University. Female NOD/ShiLtJ mice were purchased from The Jackson Laboratory, kept on a 12-hour light cycle, and fed with regular diet. The RIP-LCMV-GP mice were a gift from K. Bornfeldt's laboratory at Washington University in Seattle. ATF6 conditional knockout mice were generated with a targeting construct in which exons 8 and 9 of ATF6 were flanked by LoxP sequences. Ins2Cre mice, which have a tamoxifen-inducible Cre-mediated recombination system driven by the rat insulin 2 (*Ins2*) promoter, were purchased from The Jackson Laboratory. The genetic backgrounds of all intercrossed mouse models were verified by congenic genotyping (288 loci for C57BL/6J) with an ABI 3130 analyzer. In the RIP-LCMV-GP model, diabetes was induced with the administration of LCMV (2×10^3 PFU/ml). TUDCA (250 mg/kg) and PBS as vehicle were administered intraperitoneally to NOD and RIP-LCMV-GP mice, twice a day at 8 a.m and 8 p.m. Pancreatic sections of sXBP1 f**l**/f**l**; RIP-Cre mice were a gift from L Glimcher's laboratory at the Harvard School of Public Health.

NIH-PA Author Manuscript

NIH-PA Author Manuscript

NIH-PA Author Manuscript

Human pancreatic tissue

Paraffin-embedded pancreatic sections from diabetes-free controls and T1D patients were obtained from the Juvenile Diabetes Research Foundation (JDRF)-sponsored nPOD program (http://www.jdrfnpod.org/online-pathology.php). Sections were used for staining and quantification of expression levels of selected UPR markers.

Histological analyses

Pancreata from chemical- and vehicle-treated NOD and RIP-LCMV-GP mice were formalin-fixed and paraffin-embedded. Then, 5-μm serial sections of the pancreata were generated, and staining was performed with antibodies against insulin (Linco), glucagon, and ATF6 (Santa Cruz Biotechnology); phospho-eIF2α (Biosource); sXBP1 (in house) and GRP78 (Cell Signaling); anti-CHOP (Santa Cruz Biotechnology); and Alexa Fluor 488 and Alexa Fluor 568 (Invitrogen) according to established protocols.

Image analysis

After staining, image analysis was performed by using a custom software developed in MATLAB (The Math Works Inc.). Briefly, islet regions were identified as contiguous areas (connected pixels) of insulin staining (green channel) at or above a threshold intensity value optimized across multiple images. Mean fluorescence intensity for insulin (green channel) and for either sXBP1 or ATF6 (red channel) was calculated as the sum of intensities for all pixels divided by the number of pixels within the islet.

Immunophenotyping

Single-cell suspensions of the pancreata were prepared by collagenase digestion. Cells from pancreatic lymph nodes and spleen were prepared by physical dissociation. All stainings were started by incubating with the anti-Fcγ receptor monoclonal antibody 2.4G2. Antibodies used for subsequent stainings were anti-CD45 (30-F11) and anti-Ly6C (AL-21) (BD Pharmingen), and anti-CD3 (2C11), anti-CD4 (RM4–5), anti-CD8 (53–6.7), anti-CD25 (PC61), anti-CD11b (Ml/70), anti-CD11c (N418), anti-F4/80 (BM8), and anti-Grl (RB6–8C5) (all from BioLegend). Intracellular Foxp3 (FJK-16s) staining was performed according to eBioscience's protocol. Samples were acquired with an LSR II (BD Bioscience), and data were analyzed with FlowJo software (Tree Star Inc.).

Cell death (TUNEL) and viability (XTT) assays and insulin measurements

Serum insulin levels were measured with the Alpco ELISA kit according to the manufacturer's protocol. The Promega DeadEnd Fluorometric TUNEL system was performed on formalin-fixed, paraffin-embedded pancreatic sections according to the manufacturer's instructions. For cell viability assays, insulin-producing mouse Min6 cells (1×10^4) were seeded in 96-well microculture plates and treated with various doses of thapsigargin, cytokines, and other indicated chemicals. The J number of surviving cells was measured by the XTT assay (American Type Culture Collection) with a microplate reader. Min6 cells were J cultured in Dulbecco's modified Eagle's medium supplemented with penicillin, streptomycin, glutamine, 55 μM β-mercaptoethanol, and 10% fetal bovine serum. The cells were maintained at 37°C in 5% CO_2 atmosphere and treated with tunicamycin (1

NIH-PA Author Manuscript

NIH-PA Author Manuscript

NIH-PA Author Manuscript

to 3 μg/ml), thapsigargin (1 μM; Sigma), TUDCA (50 or 500 μg/ml; Calbiochem), and the cytokines TNF-α, IL-1β, and IFN-γ at the indicated doses (PeproTech).

Islet isolation

Islets were isolated by the Islet Resource Center at the Joslin Diabetes Center with the standard collagenase/protease digestion method. Briefly, the pancreatic duct was cannulated and distended with 4°C collagenase/protease solution with Liberase HI (Roche Diagnostics). Islets were separated from the exocrine tissue by continuous density-gradient centrifugation. Handpicked islets were cultured and counted before the experiments.

Insulin secretion assay

Min6 cells were cultured in six-well plates at 80% confluency, the growth medium was removed, and the cells were washed twice with PBS. Cells were preincubated for 30 min in 5% CO_2 at 37°C in Krebs-Ringer bicarbonate Hepes (KRBH) buffer without glucose. Incubation medium was removed, and the cells were washed once in glucose-free KRBH buffer and then incubated for 1 hour in KRBH buffer containing the indicated treatment Incubation medium was collected, and the amount of secreted insulin was determined with ELISA (Alpco, Ultrasensitive Mouse Insulin ELISA) and normalized to the total protein concentration.

Statistical analyses

Analysis of data was performed with the GraphPad Prism program (GraphPad Software). Diabetes incidence was calculated by the Kaplan-Meier estimate. Data are presented as means ± SEM or SD and analyzed with the statistical tests indicated in the text and figure legends. $P < 0.05$ was considered statistically significant.

Glucose and insulin tolerance tests and in vivo GSIS assay

Glucose tolerance tests were performed in overnight fasted mice. Mice were given glucose (2 g/kg) intraperitoneally, and then blood glucose levels were measured. Insulin tolerance tests were performed after a 6-hour daytime food withdrawal by intraperitoneal administration of recombinant human regular insulin (0.5 U/kg; Eli Lilly). In vivo GSIS tests were performed in mice after an overnight fast and by administration of glucose (2 g/kg). Serum insulin levels were quantified by ELISA (Alpco, Ultrasensitive Mouse Insulin ELISA).

Supplementary Material

Refer to Web version on PubMed Central for supplementary material.

Acknowledgments

Funding: This study was supported by a grant from JDRF to G.S.H. (17-2008-901). D.M. was supported by a grant from NIH PO1 (AI054904). D.L.E. was supported by grants from the European Union (Collaborative Projects Naimit and BetaBat in the Framework Program 7) and the Fonds National de la Recherche Scientifique. W.F. was supported by Schuylar funds.

NIH-PA Author Manuscript

NIH-PA Author Manuscript

NIH-PA Author Manuscript

REFERENCES AND NOTES

1. Lehuen A, Diana J, Zaccone P, Cooke A. Immune cell crosstalk in type 1 diabetes. Nat. Rev. Immunol. 2010; 10:501–513. [PubMed: 20577267]
2. Mathis D, Vence L, Benoist C. β-Cell death during progression to diabetes. Nature. 2001; 414:792–798. [PubMed: 11742411]
3. van Belle TL, Coppieters KT, von Herrath MG. Type 1 diabetes: Etiology immunology and therapeutic strategies. Physiol. Rev. 2011; 91:79–118. [PubMed: 21248163]
4. Eizirik DL, L Colli M, Ortis F. The role of inflammation in insulitis and β-cell loss in type 1 diabetes. Nat. Rev. Endocrinol. 2009; 5:219–226. [PubMed: 19352320]
5. Todd DJ, Lee AH, Glimcher LH. The endoplasmic reticulum stress response in immunity and autoimmunity. Nat. Rev. Immunol. 2008; 8:663–674. [PubMed: 18670423]
6. Eizirik DL, Miani M, Cardozo AK. Signalling danger: Endoplasmic reticulum stress and the unfolded protein response in pancreatic islet inflammation. Diabetologia. 2013; 56:234–241. [PubMed: 23132339]
7. Fonseca SG, Burcin M, Gromada J, Urano F. Endoplasmic reticulum stress in β-cells and development of diabetes. Curr. Opin. Pharmacol. 2009; 9:763–770. [PubMed: 19665428]
8. Scheuner D, Kaufman RJ. The unfolded protein response: A pathway that links insulin demand with β-cell failure and diabetes. Endocr. Rev. 2008; 29:317–333. [PubMed: 18436705]
9. Zhang P, McGrath B, Li S, Frank A, Zambito F, Reinert J, Gannon M, Ma K, McNaughton K, Cavener DR. The PERK eukaryotic initiation factor 2a kinase is required for the development of the skeletal system postnatal growth and the function and viability of the pancreas. Mol. Cell. Biol. 2002; 22:3864–3874. [PubMed: 11997520]
10. Harding HP, Zhang Y, Bertolotti A, Zeng H, Ron D. *Perk* is essential for translational regulation and cell survival during the unfolded protein response. Mol. Cell. 2000; 5:897–904. [PubMed: 10882126]
11. Delepine M, Nicolino M, Barrett T, Golamaully M, Lathrop GM, Julier C. EIF2AK3, encoding translation initiation factor 2-α kinase 3 is mutated in patients with Wolcott-Rallison syndrome. Nat. Genet. 2000; 25:406–409. [PubMed: 10932183]
12. Oyadomari S, Yun C, Fisher EA, Kreglinger N, Kreibich G, Oyadomari M, Harding HP, Goodman AG, Ha rant H, Garrison JL, Taunton J, Katze MG, Ron D. Cotranslocational degradation protects the stressed endoplasmic reticulum from protein overload. Cell. 2006; 126:727–739. [PubMed: 16923392]
13. Scheuner D, Song B, McEwen E, Liu C, Laybutt R, Gillespie P, Saunders T, Bonner-Weir S, Kaufman RJ. Translational control is required for the unfolded protein response and in vivo glucose homeostasis. Mol. Cell. 2001; 7:1165–1176. [PubMed: 11430820]
14. C Ladiges W, Knoblaugh SE, Morton JF, Korth MJ, L Sopher B, Baskin CR, MacAuley A, Goodman AG, LeBoeuf RC, Katze MG. Pancreatic β-cell failure and diabetes in mice with a deletion mutation of the endoplasmic reticulum molecular chaperone gene $P58^{IPK}$. Diabetes. 2005; 54:1074–1081. [PubMed: 15793246]
15. Lipson KL, Fonseca SG, Ishigaki S, Nguyen LX, Foss E, Bortell R, Rossini AA, Urano F. Regulation of insulin biosynthesis in pancreatic beta cells by an endoplasmic reticulum-resident protein kinase IRE1. Cell Metab. 2006; 4:245–254. [PubMed: 16950141]
16. Song B, Scheuner D, Ron D, Pennathur S, Kaufman RJ. *Chop* deletion reduces oxidative stress improves β cell function and promotes cell survival in multiple mouse models of diabetes. J. Clin. Invest. 2008; 118:3378–3389. [PubMed: 18776938]
17. Lee AH, Heidtman K, Hotamisligil GS, Glimcher LH. Dual and opposing roles of the unfolded protein response regulated by IRE1α and XBP1 in proinsulin processing and insulin secretion. Proc. Natl. Acad. Sci. USA. 2011; 108:8885–8890. [PubMed: 21555585]
18. Støy J, Edghill EL, Flanagan SE, Ye H, Paz VP, Pluzhnikov A, Below JE, Hayes MG, Cox NJ, Lipkind GM, Lipton RB, Greeley SA, Patch AM, Ellard S, Steiner DF, Hattersley AT, Philipson LH, Bell GI. Neonatal Diabetes International Collaborative Group, Insulin gene mutations as a cause of permanent neonatal diabetes. Proc. Natl. Acad. Sci. USA. 2007; 104:15040–15044. [PubMed: 17855560]

NIH-PA Author Manuscript

NIH-PA Author Manuscript

NIH-PA Author Manuscript

19. Wang J, Takeuchi T, Tanaka S, Kubo SK, Kayo T, Lu D, Takata K, Koizumi A, Izumi T. A mutation in the insulin 2 gene induces diabetes with severe pancreatic β-cell dysfunction in the *Mody* mouse. J. Clin. Invest. 1999; 103:27–37. [PubMed: 9884331]
20. Izumi T, Yokota-Hashimoto H, Zhao S, Wang J, Halban PA, Takeuchi T. Dominant negative pathogenesis by mutant proinsulin in the Akita diabetic mouse. Diabetes. 2003; 52:409–416. [PubMed: 12540615]
21. Colombo C, Porzio O, Liu M, Massa O, Vasta M, Salardi S, Beccaria L, Monciotti C, Toni S, Pedersen O, Hansen T, Federici L, Pesavento R, Cadario F, Federici G, Ghirri P, Arvan P, lafusco D, Barbetti F. Early Onset Diabetes Study Group of the Italian Society of Pediatric Endocrinology, Diabetes (SIEDP) Seven mutations in the human insulin gene linked to permanent neonatal/infancy-onset diabetes mellitus. J. Clin. Invest. 2008; 118:2148–2156. [PubMed: 18451997]
22. Molven A, Ringdal M, Nordbø AM, Raeder H, Støy J, Lipkind GM, Steiner DF, Philipson LH, Bergmann I, Aarskog D, Undlien DE, Joner G, Søvik; O, Norwegian Childhood Diabetes Study Group. Bell GI, Njølstad PR. Mutations in the insulin gene can cause MODY and autoantibody-negative type 1 diabetes. Diabetes. 2008; 57:1131–1135. [PubMed: 18192540]
23. Polak M, Dechaume A, Cavé H, Nimri R, Crosnier H, Sulmont V, de Kerdanet M, Scharfmann R, Lebenthal Y, Froguel P, Vaxillaire M, French ND. (Neonatal Diabetes) Study Group, Heterozygous missense mutations in the insulin gene are linked to permanent diabetes appearing in the neonatal period or in early infancy: A report from the French ND (Neonatal Diabetes) Study Group. Diabetes. 2008; 57:1115–1119. [PubMed: 18171712]
24. Størling J, Binzer J, Andersson AK, Züllig RA, Tonnesen M, Lehmann R, Spinas GA, Sandler S, Billestrup N, Mandrup-Poulsen T. Nitric oxide contributes to cytokine-induced apoptosis in pancreatic beta cells via potentiation of JNK activity and inhibition of Akt. Diabetologia. 2005; 48:2039–2050. [PubMed: 16132952]
25. Cardozo AK, Ortis F, Storling J, Feng YM, Rasschaert J, Tonnesen M, Van Eylen F, Mandrup-Poulsen T, Herchuelz A, Eizirik DL. Cytokines downregulate the sarcoendoplasmic reticulum pump Ca^{2+} ATPase 2b deplete endoplasmic reticulum Ca^{2+}leading to induction of endoplasmic reticulum stress in pancreatic β-cells. Diabetes. 2005; 54:452–461. [PubMed: 15677503]
26. Chambers KT, Unverferth JA, Weber SM, Wek RC, Urano F, Corbett JA. The role of nitric oxide and the unfolded protein response in cytokine-induced β-cell death. Diabetes. 2008; 57:124–132. [PubMed: 17928398]
27. Oyadomari S, Takeda K, Takiguchi M, Gotoh T, Matsumoto M, Wada I, Akira S, Araki E, Mori M. Nitric oxide-induced apoptosis in pancreatic β cells is mediated by the endoplasmic reticulum stress pathway. Proc. Natl. Acad. Sci. USA. 2001; 98:10845–10850. [PubMed: 11526215]
28. Dula SB, Jecmenica M, Wu R, Jahanshahi P, Verrilli GM, Carter JD, Brayman KL, Nunemaker CS. Evidence that low-grade systemic inflammation can induce islet dysfunction as measured by impaired calcium handling. Cell Calcium. 2010; 48:133–142. [PubMed: 20800281]
29. Zhang K, Kaufman RJ. From endoplasmic-reticulum stress to the inflammatory response. Nature. 2008; 454:455–462. [PubMed: 18650916]
30. Tersey SA, Nishiki Y, Templin AT, Cabrera SM, Stull ND, Colvin SC, Evans-Molina C, Rickus JL, Maier B, Mirmira RG. Islet β-cell endoplasmic reticulum stress precedes the onset of type 1 diabetes in the nonobese diabetic mouse model. Diabetes. 2012; 61:818–827. [PubMed: 22442300]
31. Marhfour I, Lopez XM, Lefkaditis D, Salmon I, Allagnat F, Richardson SJ, Morgan NG, Eizirik DL. Expression of endoplasmic reticulum stress markers in the islets of patients with type 1 diabetes. Diabetologia. 2012; 55:2417–2420. [PubMed: 22699564]
32. Bernales S, Papa FR, Walter P. Intracellular signaling by the unfolded protein response. Annu. Rev. Cell Dev. Biol. 2006; 22:487–508. [PubMed: 16822172]
33. Ozcan U, Cao Q, Yilmaz E, Lee AH, Iwakoshi NN, Ozdelen E, Tuncman G, Gorgun C, Glimcher LH, Hotamisligil GS. Endoplasmic reticulum stress links obesity insulin action and type 2 diabetes. Science. 2004; 306:457–461. [PubMed: 15486293]
34. Erbay E, Babaev VR, Mayers JR, Makowski L, Charles KN, Snitow ME, Fazio S, Wiest MM, Watkins SM, Linton MF, Hotamisligil GS. Reducing endoplasmic reticulum stress through a macrophage lipid chaperone alleviates atherosclerosis. Nat. Med. 2009; 15:1383–1391. [PubMed: 19966778]

NIH-PA Author Manuscript

NIH-PA Author Manuscript

NIH-PA Author Manuscript

35. Kensler TW, Wakabayashi N, Biswal S. Cell survival responses to environmental stresses via the Keapl-Nrf2-ARE pathway. Annu. Rev. Pharmacol. Toxicol. 2007; 47:89–116. [PubMed: 16968214]
36. Oldstone MB, Nerenberg M, Southern P, Price J, Lewicki H. Virus infection triggers insulin-dependent diabetes mellitus in a transgenic model: Role of anti-self (virus) immune response. Cell. 1991; 65:319–331. [PubMed: 1901765]
37. Ozcan U, Yilmaz E, Ozcan L, Furuhashi M, Vaillancourt E, Smith RO, Görgün CZ, Hotamisligil GS. Chemical chaperones reduce ER stress and restore glucose homeostasis in a mouse model of type 2 diabetes. Science. 2006; 313:1137–1140. [PubMed: 16931765]
38. Engin F, Hotamisligil GS. Restoring endoplasmic reticulum function by chemical chaperones: An emerging therapeutic approach for metabolic diseases. Diabetes Obes. Metab. 2010; 12(Suppl. 2): 108–115. [PubMed: 21029307]
39. Xiao C, Giacca A, Lewis GF. Sodium phenylbutyrate a drug with known capacity to reduce endoplasmic reticulum stress partially alleviates lipid-induced insulin resistance and β-cell dysfunction in humans. Diabetes. 2011; 60:918–924. [PubMed: 21270237]
40. Kars M, Yang L, Gregor MF, Mohammed BS, Pietka TA, Finck BN, Patterson BW, Horton JD, Mittendorfer B, Hotamisligil GS, Klein S. Tauroursodeoxycholic Acid may improve liver and muscle but not adipose tissue insulin sensitivity in obese men and women. Diabetes. 2010; 59:1899–1905. [PubMed: 20522594]
41. Anderson MS, Bluestone JA. The NOD mouse: A model of immune dysregulation. Annu. Rev. Immunol. 2005; 23:447–485. [PubMed: 15771578]
42. Wu AJ, Hua H, Munson SH, McDevitt HO. Tumor necrosis factor-a regulation of $CD4^+CD25^+$ T cell levels in NOD mice. Proc. Natl. Acad. Sci. U.S.A. 2002; 99:12287–12292. [PubMed: 12221281]
43. Tang Q, Henriksen KJ, Bi M, Finger EB, Szot G, Ye J, L Masteller E, McDevitt H, Bonyhadi M, Bluestone JA. In vitro-expanded antigen-specific regulatory T cells suppress autoimmune diabetes. J. Exp. Med. 2004; 199:1455–1465. [PubMed: 15184499]
44. Sgouroudis E, Piccirillo CA. Control of type 1 diabetes by $CD4^+Foxp3^+$ regulatory T cells: Lessons from mouse models and implications for human disease. Diabetes Metab. Res. Rev. 2009; 25:208–218. [PubMed: 19214972]
45. Staeva TP, Chatenoud L, Insel R, Atkinson MA. Recent lessons learned from prevention and recent-onset type 1 diabetes immunotherapy trials. Diabetes. 2013; 62:9–17. [PubMed: 23258904]
46. Mathews CE, Graser RT, Savinov A, Serreze DV, Leiter EH. Unusual resistance of ALR/Lt mouse |3 cells to autoimmune destruction: Role for β celI-expressed resistance determinants. Proc. Natl. Acad. Sci. USA. 2001; 98:235–240. [PubMed: 11136257]
47. Yang P, Li M, Guo D, Gong F, Adam BL, Atkinson MA, Wang CY. Comparative analysis of the islet proteome between NOD/Lt and ALR/Lt mice. Ann. N. Y. Acad. Sci. 2008; 1150:68–71. [PubMed: 19120270]
48. Li H, Korennykh AV, Behrman SL, Walter P. Mammalian endoplasmic reticulum stress sensor IRE1 signals by dynamic clustering. Proc. Natl. Acad. Sci. USA. 2010; 107:16113–16118. [PubMed: 20798350]
49. Lin JH, Li H, Yasumura D, Cohen HR, Zhang C, Panning B, Shokat KM, Lavail MM, Walter P. IRE1 signaling affects cell fate during the unfolded protein response. Science. 2007; 318:944–949. [PubMed: 17991856]
50. Toko H, Takahashi H, Kayama Y, Okada S, Minamino T, Terasaki F, Kitaura Y, Komuro I. ATF6 is important under both pathological and physiological states in the heart. J. Mol. Cell. Cardiol. 2010; 49:113–120. [PubMed: 20380836]
51. Martindale JJ, Fernandez R, Thuerauf D, Whittaker R, Gude N, Sussman MA, Glembotski CC. Endoplasmic reticulum stress gene induction and protection from ischemia/reperfusion injury in the hearts of transgenic mice with a tamoxifen-regulated form of ATF6. Circ. Res. 2006; 98:1186–1193. [PubMed: 16601230]
52. Wang Y, Vera L, Fischer WH, Montminy M. The CREB coactivator CRTC2 links hepatic ER stress and fasting gluconeogenesis. Nature. 2009; 460:534–537. [PubMed: 19543265]

NIH-PA Author Manuscript

NIH-PA Author Manuscript

NIH-PA Author Manuscript

53. Teodoro T, Odisho T, Sidorova E, Volchuk A. Pancreatic β-cells depend on basal expression of active ATF6α-p50 for cell survival even under nonstress conditions. Am. J. Physiol. Cell Physiol. 2012; 302:C992–C1003. [PubMed: 22189555]
54. Skyler JS. Prediction and prevention of type 1 diabetes: Progress problems and prospects. Clin. Pharmacol. Ther. 2007; 81:768–771. [PubMed: 17392722]
55. Skyler JS. Immune intervention for type 1 diabetes mellitus. Int. J. Clin. Pract. Suppl. 2011; 170:61–70. [PubMed: 21323814]
56. Zhang L, Eisenbarth GS. Prediction and prevention of type 1 diabetes mellitus. J. Diabetes. 2011; 3:48–57. [PubMed: 21073664]
57. Ziegler AG, Nepom GT. Prediction and pathogenesis in type 1 diabetes. Immunity. 2010; 32:468–478. [PubMed: 20412757]
58. Hofmann AF. The continuing importance of bile acids in liver and intestinal disease. Arch. Intern. Med. 1999; 159:2647–2658. [PubMed: 10597755]
59. Rubin RA, Kowalski TE, Khandelwal M, Malet PF. Ursodiol for hepatobiliary disorders. Ann. Intern. Med. 1994; 121:207–218. [PubMed: 8017748]
60. Rewers M, Gottlieb P. Immunotherapy for the prevention and treatment of type 1 diabetes: Human trials and a look into the future. Diabetes Care. 2009; 32:1769–1782. [PubMed: 19794002]

NIH-PA Author Manuscript
NIH-PA Author Manuscript
NIH-PA Author Manuscript

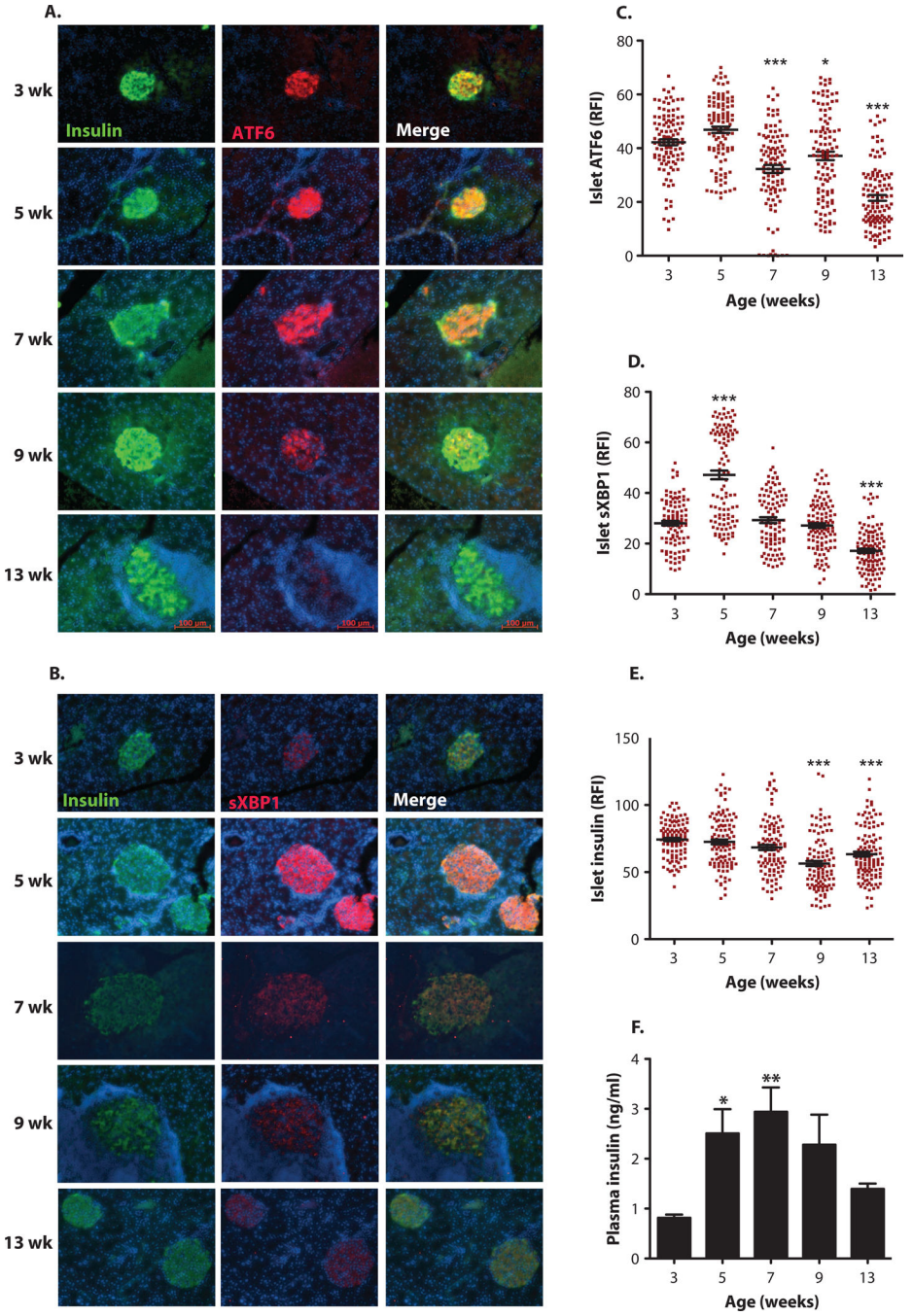

Fig. 1. Time-course detection of altered expression of UPR mediators in the islets of NOD mice

Female NOD mice (*n* = 14 for each group) were sacrificed at 3,5,7,9, and 13 weeks of age. (**A** and **B**) Immunofluorescence assays were performed on the pancreatic sections by costaining with either (A) anti-ATF6 antibody (red) or (B) anfrsXBPI (red) and anti-insulin (green) antibodies. The cell nuclei were counterstained with 4',6-diamidino-2-phenylindole (DAPI) (blue). (**C** to **E**) Relative fluorescence intensity (RFI) for (C) ATF6, (D) sXBPI, and (E) insulin was calculated by MATLAB (15 to 25 islets per animal per time point). (F) Serum insulin levels of NOD mice (*n* = 14) were measured by enzyme-linked

immunosorbent assay (EUSA). All data are presented as means ± SEM, with statistical analysis performed by one-way analysis of variance (ANOVA) (***$P < 0.001$; **$P < 0.005$; *$P < 0.05$).

NIH-PA Author Manuscript
NIH-PA Author Manuscript
NIH-PA Author Manuscript

NIH-PA Author Manuscript
NIH-PA Author Manuscript
NIH-PA Author Manuscript

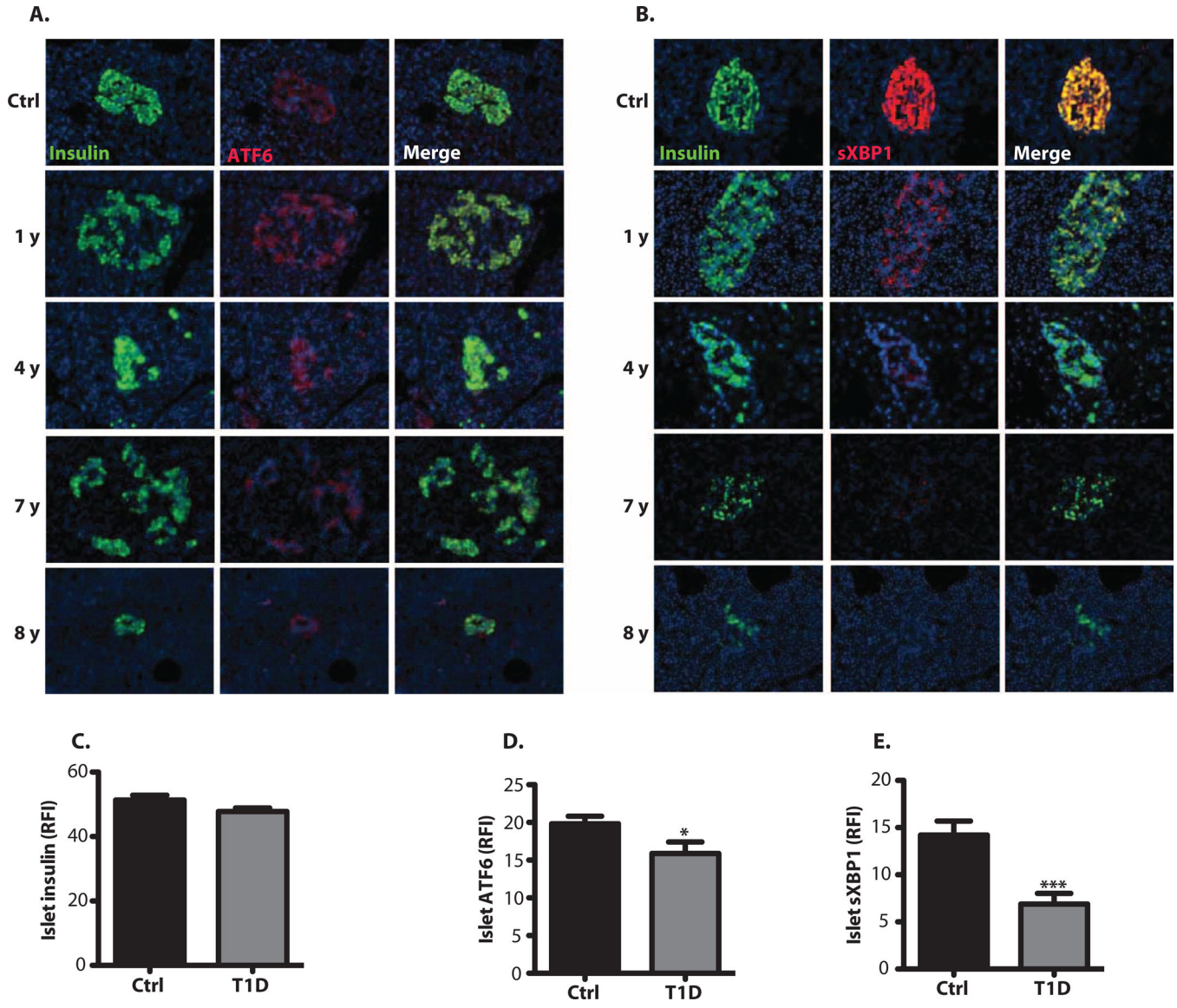

Fig. 2. Dysregulated UPR expression in the β cells of human T1D patients

(**A** and **B**) Pancreatic sections from nondiabetic (Ctrl) and diabetic female patients were grouped and costained with either (A) anti-ATF6 (red) and anti-insulin (green) or (B) anti-sXBPI (red) and anti-insulin (green). The cell nuclei were counterstained with DAPI (blue). (**C** to **E**) Relative fluorescence intensity (RFI) of (C) insulin, (D) sXBPI, and (E) ATF6 in the pancreatic sections was calculated on 15 to 25 islets per time point. All data are presented as means ± SEM, with statistical analysis performed by one-way ANOVA (***$P < 0.001$; **$P < 0.005$; *$P < 0.05$).

NIH-PA Author Manuscript
NIH-PA Author Manuscript
NIH-PA Author Manuscript

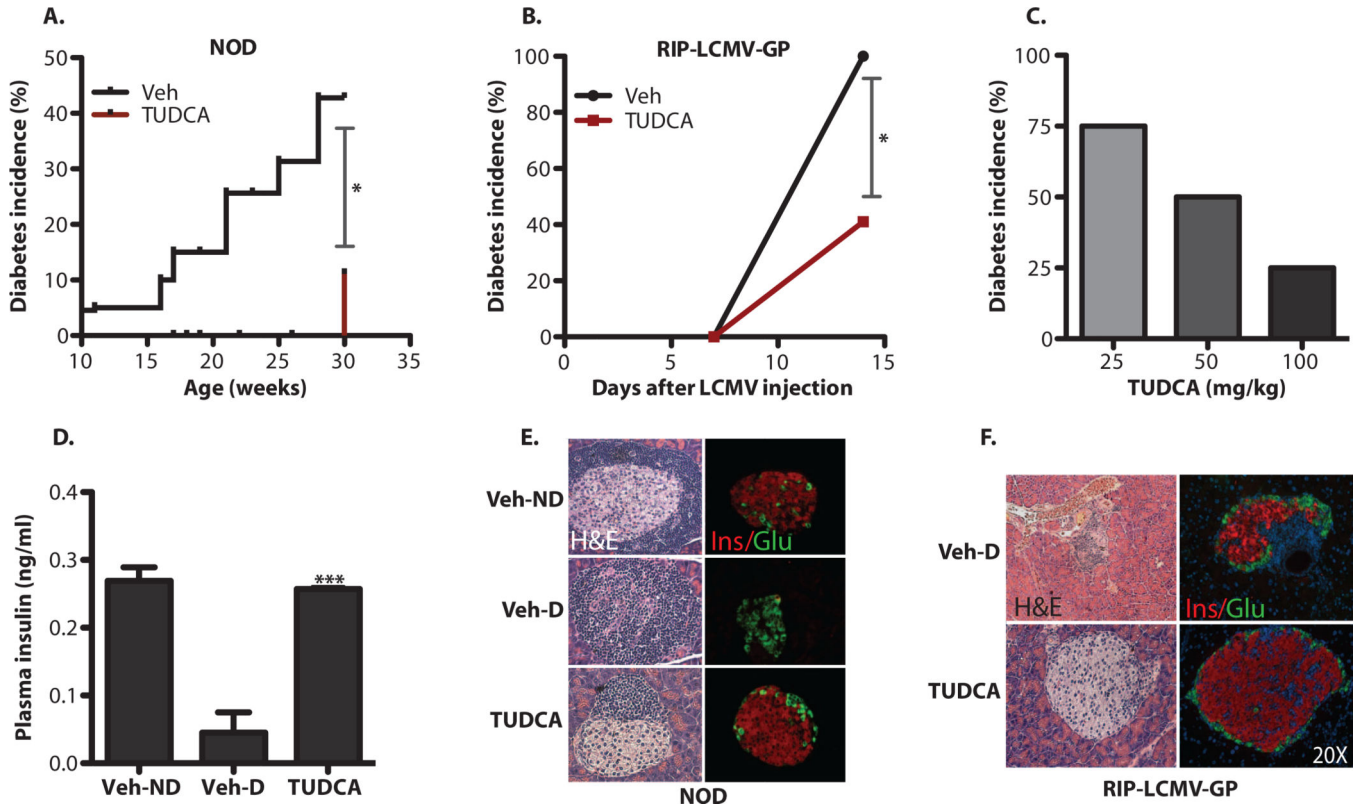

Fig. 3. Decreased diabetes incidence in NOD and RIP-LCMV-GP mice upon treatment with TUDCA

(A) Female NOD mice (n = 20 in each group) received twice-daily intraperitoneal injections of TUDCA (250 mg/kg) or vehicle (PBS) starting at 10 weeks of age, and blood glucose levels were monitored up to 30 weeks of age. (**B**) The same treatment was applied to RIP-LCMV-GP mice (n = 12) right after induction of diabetes with LCMV [2×10^3 plaque-forming units (PFU)/ml], and blood glucose levels were monitored for 2 weeks. (**C**) Reduction of diabetes incidence with various doses of TUDCA in RIP-LCMV-GP animals was determined after 2 weeks of treatment. (**D**) Serum insulin levels were measured by ELISA in vehicle (PBS)–treated NOD mice without diabetes (Veh-ND), vehicle-treated NOD mice with diabetes (Veh-D), or TUDCA-treated NOD mice (TUDCA). (**E**) Pancreatic sections from vehicle (PBS)– or TUDCA-treated NOD mice (30 weeks of age) were stained with H&E. Representative images of vehicle-treated mice without diabetes (Veh-ND) are presented in the upper panel. TUDCA treatment (lower panel) resulted in better-preserved islet morphology and less lymphocytic infiltration compared to vehicle-treated diabetic (Veh-D) NOD mice (middle panel). Immunofluorescence analysis of these islets with anti-insulin and anti-glucagon antibodies indicated the presence of functional β and α cells in TUDCA-treated mice. (**F**) Pancreatic sections from vehicle-treated (PBS) (upper panel) or TUDCA-treated (lower panel) RIP-LCMV-GP mice were stained with H&E (left panels) or examined by insulin and glucagon immunofluorescence analysis (right panels). Data are presented as means ± SEM, with statistical analysis performed by the Kaplan-Meier estimate (A), χ^2test (B), or one-way ANOVA (D) (***P < “ 0.001; *P< 0.05).

NIH-PA Author Manuscript
NIH-PA Author Manuscript
NIH-PA Author Manuscript

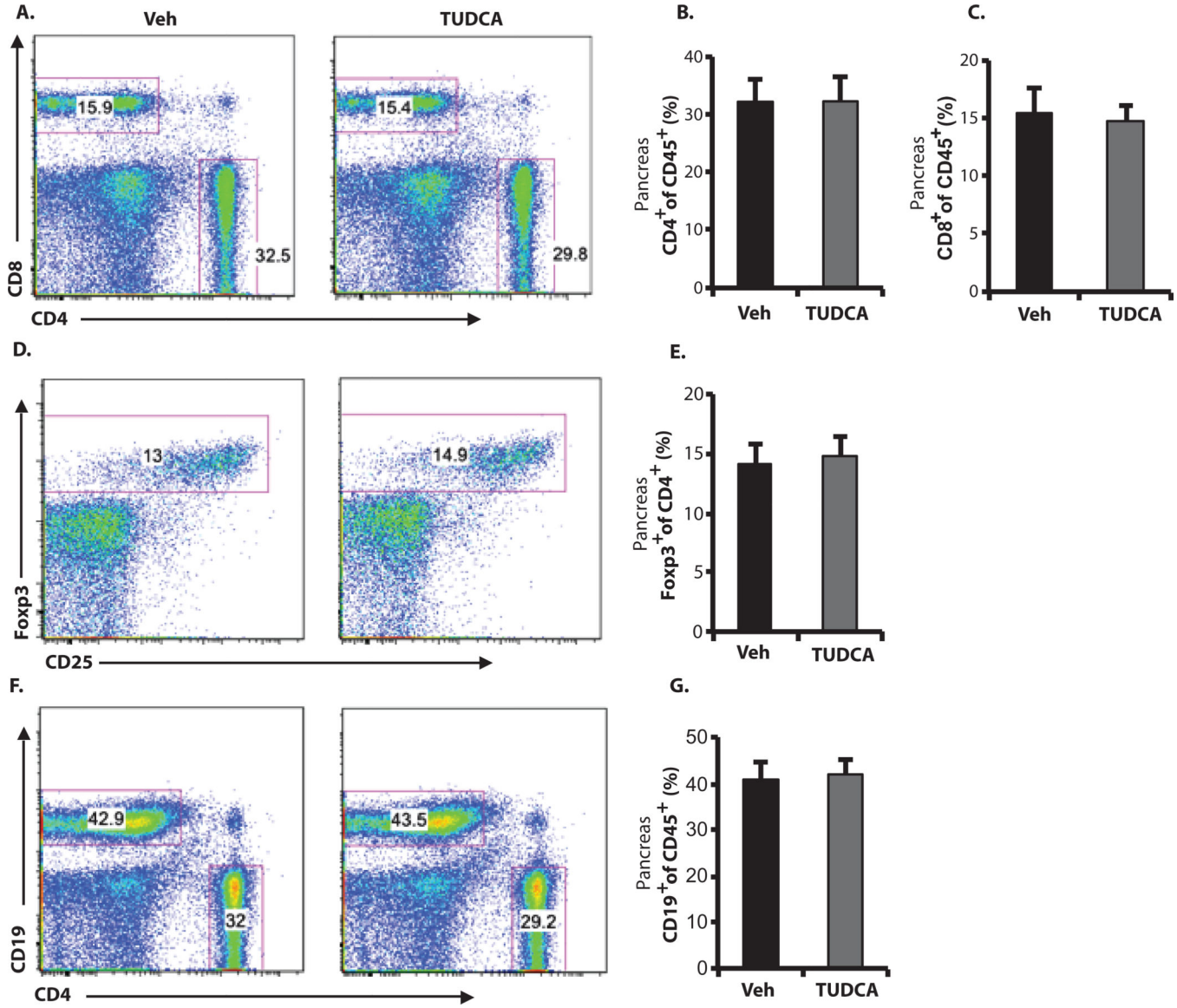

Fig. 4. Lack of TUDCA-induced alterations in immune cell populations in NOD pancreata

Ten-week-old female NOD mice were treated with TUDCA (500 mg/kg per day) or vehicle (PBS) (n = 7 in each group) for 4 weeks. Each pancreas was isolated and dispersed, and cells were analyzed by flow cytometry after staining with antibodies against CD45, CD4, CD8, CD19, CD25, and Foxp3. Cells were pregated as $CD45^+$. (**A**) Fractions of $CD4^+$ or $CD8^+$ T cells in representative dot plots. (**B** and **C**) Summary data for all mice. (**D** and **E**) Corresponding dot plots and summary data for $Foxp3^+$ cells pregated as $CD45^+$ and $CD4^+$. (**F** and **G**) Corresponding dot plots and summary data for CD19+ B cells pregated as CD45+. Student′s t test did not show any significant statistical difference between vehicle- and TUDCA-treated cells.

NIH-PA Author Manuscript
NIH-PA Author Manuscript
NIH-PA Author Manuscript

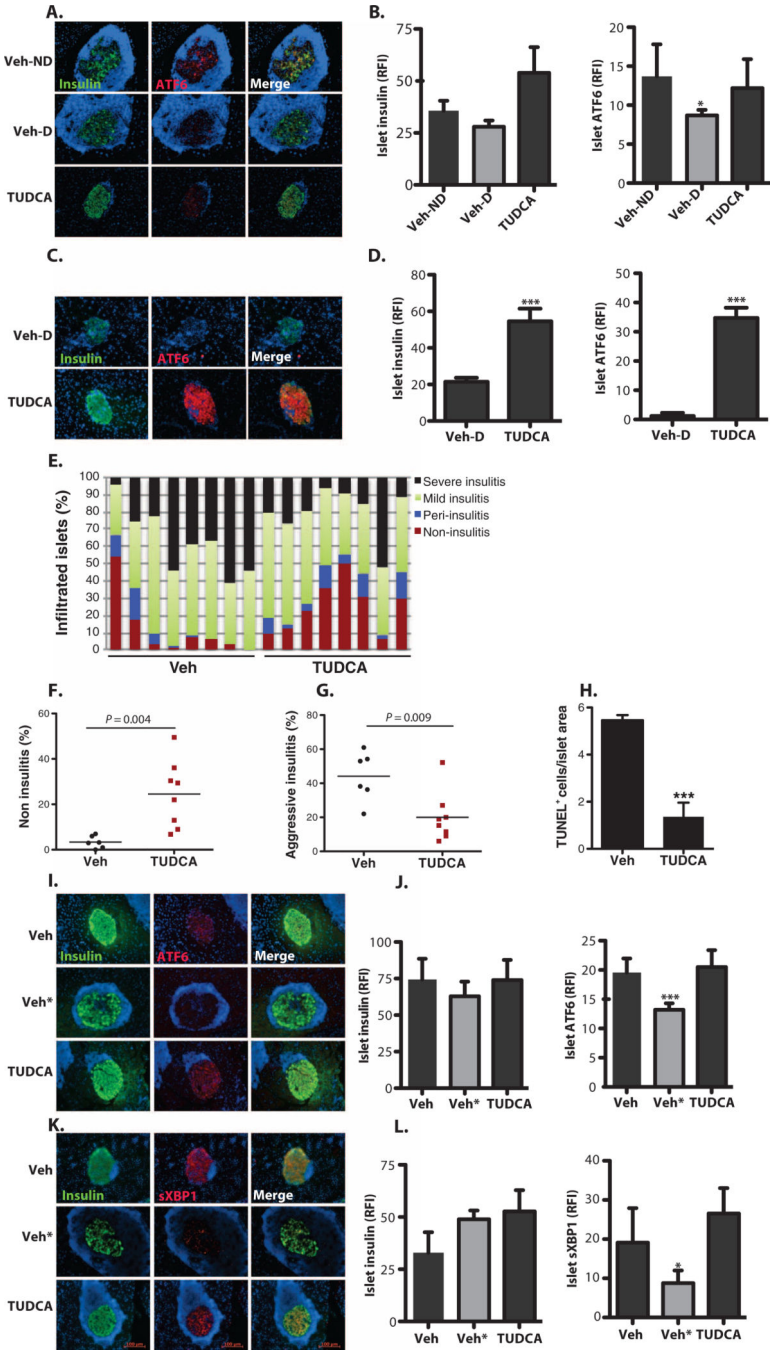

Fig. 5. Recovery of adaptive UPR mediators in islets of TUDCA-treated NOD and RIP-LCMV-GP mice

(**A**) Pancreatic sections from 30-week-old vehicle-treated non-diabetic (Veh-ND) (*n* = 5), vehicle-treated diabetic (Veh-D) (*n* = 4), and TUDCA-treated (*n* = 9) NOD mice stained with anti-ATF6 (red) and anti-insulin (green). The cell nuclei were counterstained with DAPI (blue). (**B**) Quantification of relative fluorescence intensity (RFI) of insulin and ATF6 in the islets of vehicle-treated nondiabetic (Veh-ND), vehicle-treated diabetic (Veh-D), and TUDCA-treated NOD mice. (**C**) Pancreatic sections from 16-week-old vehicle-treated

NIH-PA Author Manuscript

NIH-PA Author Manuscript

NIH-PA Author Manuscript

diabetic (upper panel) or TUDCA-treated RIP-LCMV-GP (lower panel) mice stained with anti-ATF6 (red) and anti-insulin (green). The cell nuclei were counterstained with DAPI (blue). (**D**) Quantification of islet fluorescence intensity of insulin and ATF6 in vehicle- and TUDCA-treated mice. (**E**) Insulitis scoring was performed on the H&E-stained step sections of the pancreata from 10-week-old NOD mice treated with either PBS vehicle (n = 8) or TUDCA (*n* = 8) for 4 weeks. (**F**) Vehicle- or TUDCA-treated NOD mouse islets were quantified for the presence of islets that did not display insulitis (**P* < 0.05). (**G**) Vehicle- or TUDCA-treated NOD mouse islets were quantified for the presence of the islets that displayed aggressive insulitis. TUDCA-treated mice had significantly lower percentages of islets with aggressive insulitis. (**H**) Pancreata from control and TUDCA-treated animals were assessed for apoptosis with the TUNEL assay. (**I** and **K**) Vehicle- and TUDCA-treated normoglycemic NOD mouse pancreata were costained with (I) anti-ATF6 (red) or (K) anti-sXBPI (red) and anti-insulin (green) antibodies. Vehicle-treated animals were grouped according to their insulitis scoring [determined in (E)], and the group with the lowest insulitis scoring is shown in the upper panel. Vehicle-treated animals with severe insulitis were indicated as Veh* (middle panel). The staining of TUDCA-treated animals is shown in the lower panel. Relative fluorescence intensity analysis indicated significantly reduced (**J**) ATF6 and (**L**) sXBPI expression in the group with higher insulitis scoring, whereas TUDCA-treated animals showed a similar degree of expression to the animals with lower insulitis scoring. Insulin expression in the islets was the same in all groups (J and L). Data are presented as means ± SEM, with statistical analysis performed by one-way ANOVA (B, J, and L) or by Student′s *t* test (D and F to H) (****P* < 0.001; **P* < 0.05).

NIH-PA Author Manuscript
NIH-PA Author Manuscript
NIH-PA Author Manuscript

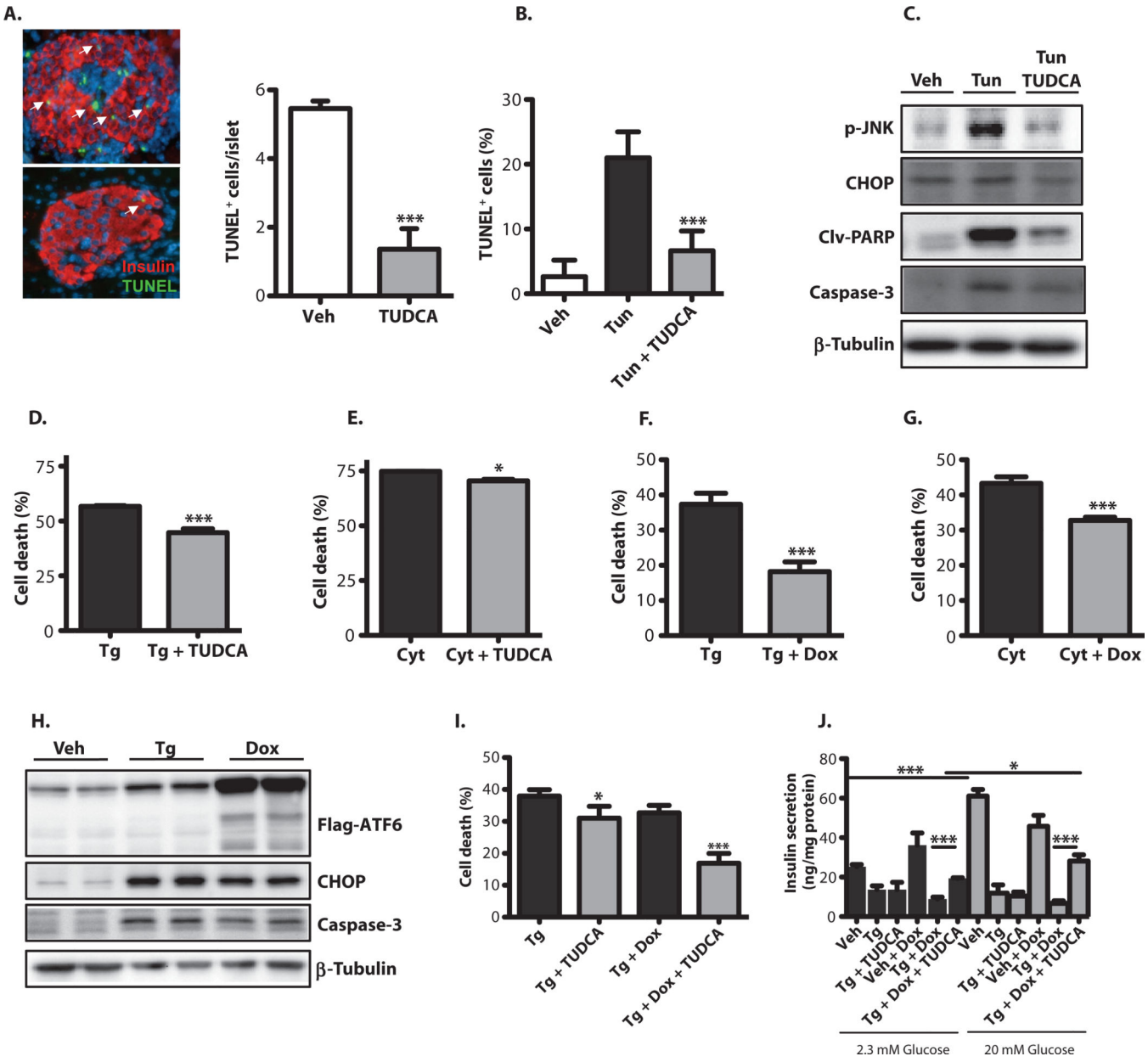

Fig. 6. TUDCA-driven protection of β cells against cytokine- and ER stress-induced cell death

(**A**) Pancreatic sections from vehicle- or TUDCA-treated RIP-LCMV-GP mice were assessed for apoptosis with the TUNEL assay. White arrowheads indicate TUNEL-positive cells. (**B**) Min6 cells were treated with tunicamycin (1 μg/ml) for 18 hours with or without TUDCA, and cell death was determined with the TUNEL assay. (**C**) Min6 cells were treated as in (B),and markers of apoptosis were analyzed by Western blotting with anti-p-JNK, anti-CHOP, anti-cleaved PARP, and anti-caspase-3 antibodies. (**D**) Min6 cells were treated with 1 μM thapsigargin with or without 250 μM TUDCA for 24 hours. Cell viability was assessed with the XTT {sodium 3′-[(1-phenyl amino-carbonyl)-3,4-tetrazolium]-bis(4-methoxy-6-nitro)benzene sulfonic acid hydrate} assay. (**E**) Min6 cells were treated with a cytokine cocktail with or without 250 μM TUDCA for 40 hours. Cell viability was assessed with the

NIH-PA Author Manuscript

NIH-PA Author Manuscript

NIH-PA Author Manuscript

XTT assay. (**F**) Min6 cells transduced with a lentivirus expressing 3XFIag-tagged ATF6. After treatment of Min6 cells with 3 μM doxycycline for 24 hours, 1 μM thapsigargin was added to the medium for 24 hours, and cell viability was determined with the X**TT** assay. (**G**) Transduced Min6 cells were treated with 3 μM doxycycline for 24 hours, the cytokine cocktail was added to the medium for 24 hours, and cell viability was determined with the XTT assay. (**H**) Transduced Min6 cells were treated with 3 μM doxycycline for 24 hours, 1 μM thapsigargin was added to the medium, and incubation was continued for an additional 24 hours. Apoptosis markers were analyzed by Western blotting with anti-CHOP and anti-caspase-3 antibodies. (**I**) Transduced Min6 cells were treated with either vehicle or 0.1 μM doxycycline for 24 hours. Thapsigargin (1 μM) was added to the medium, incubation was continued for an additional 24 hours in the presence or absence of 30 μM TUDCA, and then cell viability was determined with the XTT assay. (**J**) Cultured Min6 cells were transduced with a lentivirus expressing 3XFIag-tagged ATF6 and then treated with either vehicle or 3 μM doxycycline for 24 hours. Thapsigargin (1 μM) was then added to the medium, incubation was continued for an additional 24 hours in the presence or absence of 50 μM TUDCA, and GSIS under low- and high-glucose conditions was determined by insulin ELISA Results were replicated in three independent experiments. Data are presented as means ± SEM, with statistical analysis performed by Student′s f test (A, B, and D to G) or one-way ANOVA (I and J) (***$P < 0.001$; *$P < 0.05$).

NIH-PA Author Manuscript
NIH-PA Author Manuscript
NIH-PA Author Manuscript

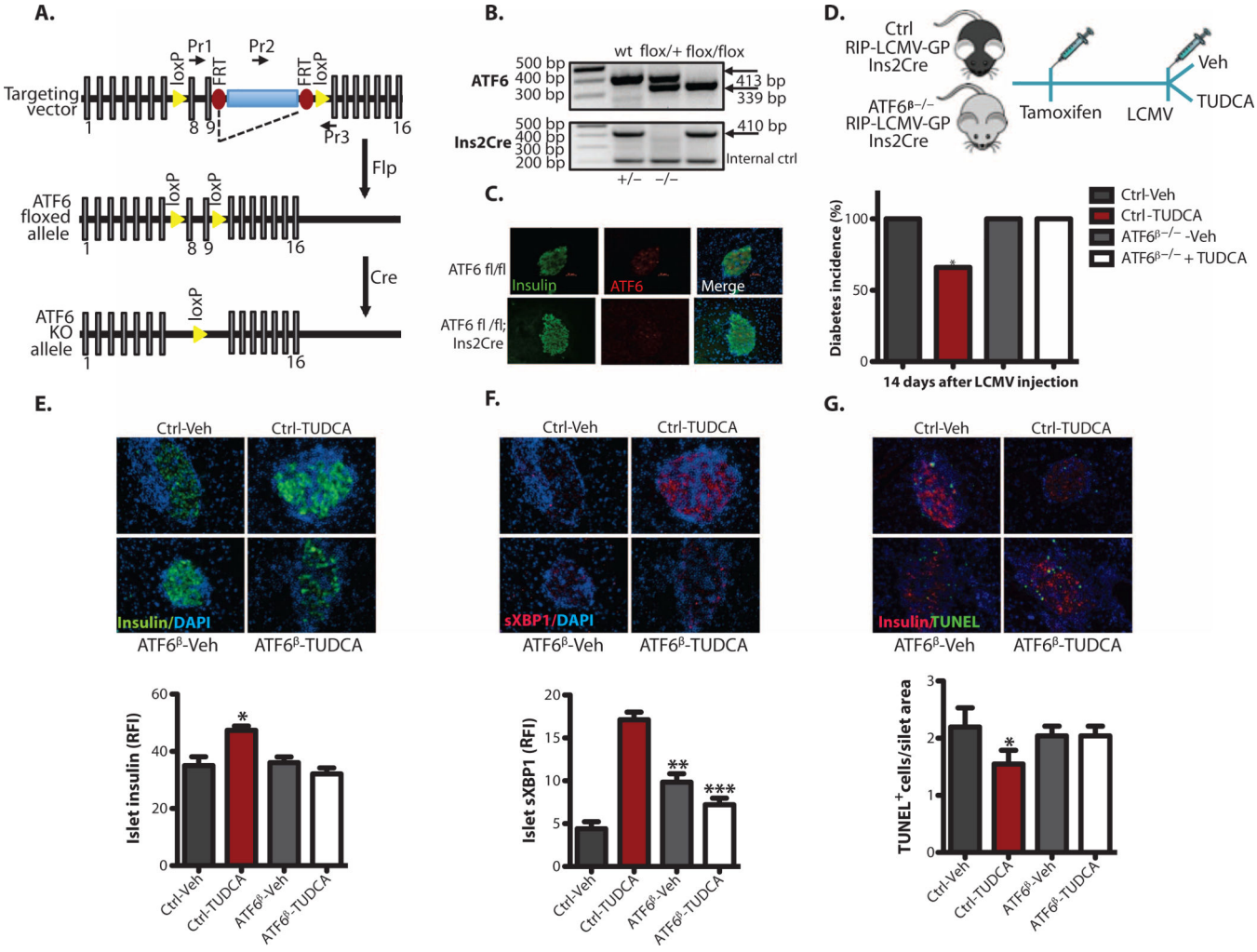

Fig. 7. TUDCA protection of β cells through the ATF6 branch of the UPR

(A) Schematic representation of a targeting vector used for the generation of conditional β cell-specific ATF6-deficient ($ATF6^{\beta-/-}$) mice. (**B**) Genotyping of control and $ATF6^{\beta-/-}$ mice was performed with tail DNA. (**C**) An immunofluorescence assay was performed to validate the tissue-specific deletion of *ATF6*. (**D**) Vehicle (PBS) or TUDCA (250 mg/kg twice daily via intraperitoneal injection) was applied to ATF6 wild-type (wt) control mice or $ATF6^{\beta-/-}$ RIP-LCMV-GP mice immediately after induction of diabetes with LCMV (2×10^3 PFU/ml), and blood glucose levels were monitored for 2 weeks. (**E**) Female control and $ATF6^{\beta-/-}$; RIP-LCMV-GP; lns2Cre mice were treated with either vehicle or TUDCA ($n = 4$ each group) for 2 weeks. (**F**) The mice were then sacrificed, and the relative immunofluorescence intensity (RFI) of insulin (green) or sXBPI (red) expression (20 to 30 islets per animal per group) was quantified by MATLAB. (**G**) Pancreatic sections from vehicle- or TUDCA-treated control and $ATF6^{\beta-/-}$ RIP-LCMV-GP mice ($n = 4$ each group, 20 to 30 islets per group) were examined for apoptosis with the TUNEL assay. All data are presented as means ± SEM, with statistical analysis performed by one-way ANOVA (***$P < 0.001$; **$P < 0.005$; *$P < 0.05$).

NIH-PA Author Manuscript NIH-PA Author Manuscript NIH-PA Author Manuscript

Sci Transl Med. Author manuscript; available in PMC 2014 September 19.

Table 1

Information on the T1D and control nondiabetic donors

Pancreatic sections were obtained from nPOD for immunofluorescence analysis of UPR mediators.

Patient	Age (years)	Sex	Ethnicity	Duration of diabetes (years)	AutoAb	Histology
Ctrl	0.5	Female	African American	N/A	Negative	Normal islet
Ctrl	2.9	Male	African American	N/A	Negative	Normal islet
Ctrl	17.8	Male	Caucasian	N/A	Negative	Normal islet, few with vascular stasis
Ctrl	19.2	Male	Caucasian	N/A	Negative	Normal islet
Ctrl	32	Female	Caucasian	N/A	Negative	Normal islet, low Ki67
Ctrl	59	Female	Caucasian	N/A	Negative	Normal islet
T1D	13.1	Female	Caucasian	1	mIAA$^+$	Ins$^+$ (reduced)/Gluc$^+$ islets; insulitis
T1D	33.9	Female	Caucasian	4	Negative	Ins$^+$/Gluc$^+$ islets; increased acinar Ki67
T1D	14.2	Male	Caucasian	4	mIAA$^+$	Ins$^+$ islets in lobules with moderate to severe adipose infiltrates
T1D	31.2	Male	Caucasian	5	GADA$^+$, IA2A$^+$, ZnT8A$^+$, mIAA$^+$	Ins$^+$/Gluc$^+$ islets (much decreased); insulitis; chronic pancreatitis
T1D	22.8	Female	Caucasian	7	IA-2A$^+$, mIAA$^+$	Ins$^+$ islet (few); occ. Ki67$^+$ islet cell; insulitis
T1D	22.9	Male	African American	7	No serum available	Ins$^+$ islet of various sizes; acinar atrophy and fibrosis
T1D	18.8	Female	Caucasian	8	IA-2A$^+$, ZnT8A$^+$	Ins$^+$ islet in occ. lobule, Ins$^-$/Gluc$^+$ islet
T1D	20.3	Male	Caucasian	13	mIAA$^+$	Ins$^+$ (very reduced)/Gluc$^+$ variable within lobules, islet atrophy
T1D	31.4	Male	Hispanic	15	Negative	Ins$^+$ islet; mild to moderate chronic pancreatitis
T1D	50	Female	Caucasian	20	mIAA$^+$	Ins$^+$ islet, insulitis, Ins$^-$/Gluc$^+$ islets

Ins, insulin; Gluc, glucagon; Ab, antibody; N/A, not applicable.